Cell Metabolism
Article

RBP4 Disrupts Vitamin A Uptake Homeostasis in a STRA6-Deficient Animal Model for Matthew-Wood Syndrome

Andrea Isken,[1] Marcin Golczak,[2] Vitus Oberhauser,[1] Silke Hunzelmann,[1,2] Wolfgang Driever,[1] Yoshikazu Imanishi,[2] Krzysztof Palczewski,[2,*] and Johannes von Lintig[1,2,*]
[1]Institut für Biologie 1, Albert-Ludwigs-Universität Freiburg, 79104 Freiburg, Germany
[2]Department of Pharmacology, Case Western Reserve University School of Medicine, Cleveland, OH 44106-4965, USA
*Correspondence: kxp65@case.edu (K.P.), lintig@biologie.uni-freiburg.de (J.v.L.)
DOI 10.1016/j.cmet.2008.01.009

SUMMARY

The cellular uptake of vitamin A from its RBP4-bound circulating form (holo-RBP4) is a homeostatic process that evidently depends on the multidomain membrane protein STRA6. In humans, mutations in *STRA6* are associated with Matthew-Wood syndrome, manifested by multisystem developmental malformations. Here we addressed the metabolic basis of this inherited disease. STRA6-dependent transfer of retinol from RBP4 into cultured NIH 3T3 fibroblasts was enhanced by lecithin:retinol acyltransferase (LRAT). The retinol transfer was bidirectional, strongly suggesting that STRA6 acts as a retinol channel/transporter. Loss-of-function analysis in zebrafish embryos revealed that Stra6 deficiency caused vitamin A deprivation of the developing eyes. We provide evidence that, in the absence of Stra6, holo-Rbp4 provokes nonspecific vitamin A excess in several embryonic tissues, impairing retinoic acid receptor signaling and gene regulation. These fatal consequences of Stra6 deficiency, including craniofacial and cardiac defects and microphthalmia, were largely alleviated by reducing embryonic Rbp4 levels by morpholino oligonucleotide or pharmacological treatments.

INTRODUCTION

The biological importance of retinoids (vitamin A and its derivatives) for vertebrate development has long been known, because both deprivation of and excessive exposure to retinoids cause major embryonic abnormalities (reviewed by Mark et al., 2006). Vitamin A is the precursor of at least two critical metabolites: 11-*cis*-retinal, the chromophore of visual G protein-coupled receptors (Palczewski, 2006), and all-*trans*-retinoic acid (RA). RA regulates gene expression via heterodimeric nuclear receptors consisting of both RA receptors (RARs) and retinoid X receptors (RXRs) (Giguere et al., 1987; Petkovich et al., 1987). Both are ligand-dependent transcription factors belonging to the superfamily of nuclear hormone receptors (Chambon, 1996).

A prerequisite for initiation of retinoid-dependent physiological processes is the coordinated production of biologically active retinoids from circulating precursors. To achieve this, cells and tissues must be adequately supplied with this vitamin throughout their life cycle. All-*trans*-retinol bound to the retinol-binding protein RBP4 (holo-RBP4) serves as the major transport mode for vitamin A in the blood (Blomhoff et al., 1990). It has long been postulated that cellular retinol uptake from holo-RBP4 is a facilitated, protein-mediated process (for review, see Blaner, 2007). Recently, it has been suggested that the multitransmembrane domain protein STRA6 acts as the long-sought RBP4 receptor. In cell cultures, STRA6 specifically binds to holo-RBP4 and mediates the cellular uptake of retinol (Kawaguchi et al., 2007). In mammals, STRA6 is expressed in a variety of embryonic and adult cells and tissues (Bouillet et al., 1997; Kawaguchi et al., 2007). Mutations of *STRA6* in humans cause the fatal Matthew-Wood syndrome, characterized by pleiotropic, multisystem malformations that include cardiac deformities and ocular defects (Golzio et al., 2007; Pasutto et al., 2007). These dramatic consequences of STRA6 deficiency were unexpected because RBP4-deficient patients display only a mild clinical phenotype that includes night blindness and modest retinal dystrophy (Biesalski et al., 1999). RBP4-deficient mice also are phenotypically normal except for a visual impairment early in life that can be corrected during adolescence by maintaining them on a vitamin A-rich diet (Quadro et al., 1999). The discrepancy between the STRA6- and RBP4-deficient phenotypes led to the speculation that STRA6 functions in an additional unknown process (Blaner, 2007). To address this question, we further characterized the function of STRA6 in cell culture and established a zebrafish model to elucidate the biochemical and developmental consequences of STRA6 deficiency.

RESULTS

STRA6 Enhances Retinol Uptake in NIH 3T3 Cells

To confirm that STRA6 mediates the cellular uptake of vitamin A, we established stable NIH 3T3 cell lines expressing human STRA6 and human lecithin:retinol acyltransferase (LRAT). To obtain a cell line expressing both proteins, we introduced a human *STRA6* gene construct into NIH 3T3 cells expressing human LRAT. Expression of STRA6 was confirmed by immunoblotting and immunohistochemistry. ID4-tagged STRA6 localized to the plasma membrane and, to some extent, to the

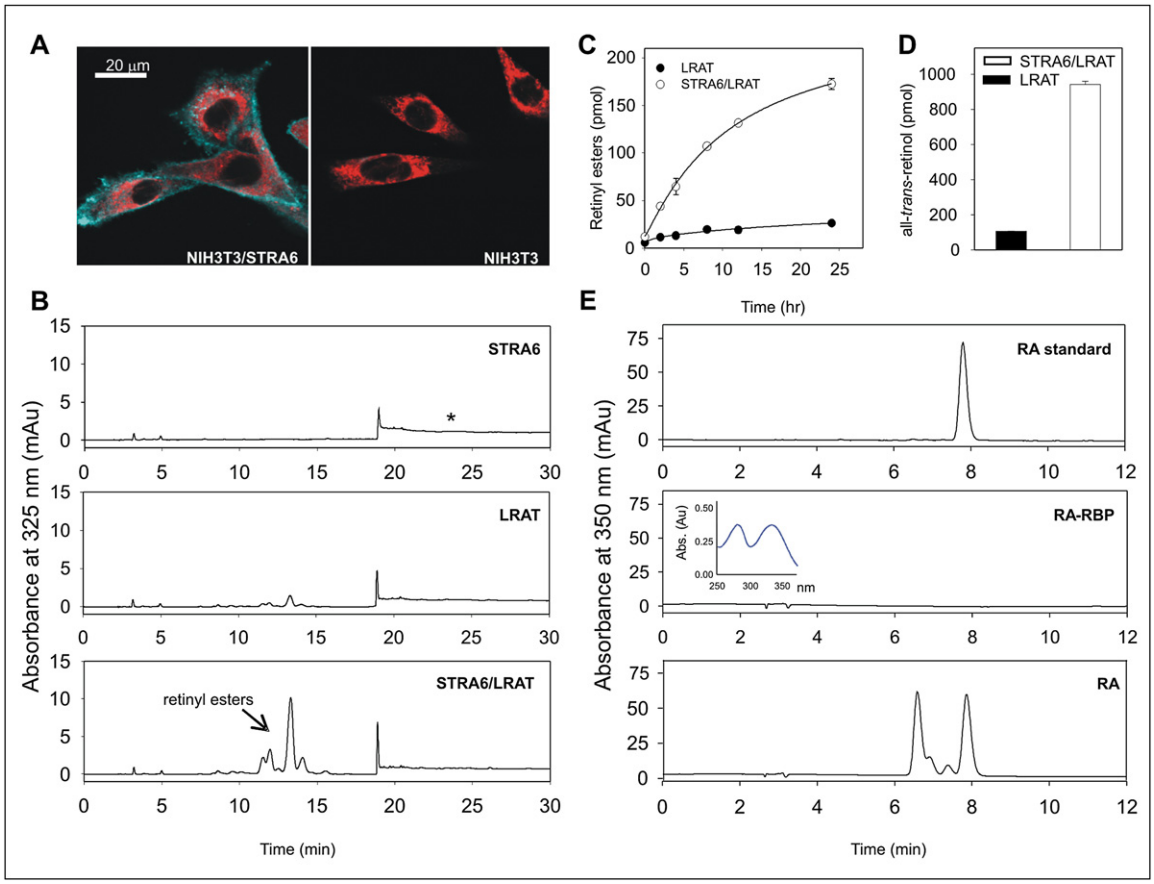

Figure 1. STRA6-Dependent Uptake and Release of Retinoids

(A) Subcellular localization of STRA6 tagged with 1D4 epitope (blue) stably expressed in NIH 3T3 cells was determined by immunohistochemistry and confocal microscopy; calreticulin was detected by anti-calreticulin polyclonal antibody (red). Scale bar = 20 μm.

(B) Chromatograms representing retinoid composition of STRA6-, LRAT-, and STRA6/LRAT-expressing cells after incubation with 8 μM holo-RBP4. Asterisk indicates the position at which all-*trans*-retinol migrates.

(C) Time course of retinol uptake. LRAT- and STRA6/LRAT-expressing cells were incubated with 8 μM holo-RBP4. Retinoid content of the cells was determined at the time points indicated. Values represent the mean ± SD of three independent experiments.

(D) STRA6-dependent release of retinol. Cells were incubated with 10 μM all-*trans*-retinol for 16 hr prior to this experiment. Cells then were washed with PBS, and fresh medium containing 8 μM apo-RBP4 was added. After 16 hr, the medium was collected and retinoid composition was determined by HPLC. Values represent the mean ± SD of three independent experiments.

(E) Retinoic acid uptake is not STRA6 dependent. Apo-RBP was loaded with all-*trans*-retinoic acid (RA) and purified by fast protein liquid chromatography (FPLC). Efficiency of RA loading was confirmed by absorption spectroscopy (inset). NIH 3T3 cells stably expressing STRA6 and LRAT were incubated with 8 μM RA-RBP4 or 8 μM RA overnight. Retinoid composition was determined by reverse-phase chromatography.

endoplasmic reticulum as shown by the merged image with calreticulin (Figure 1A). To determine STRA6-mediated retinol uptake from holo-RBP4, we incubated the different cell lines with 8 μM holo-RBP4 for 16 hr and then analyzed their retinoid content by high-pressure liquid chromatography (HPLC). The chromatograms revealed that retinol uptake from holo-RBP4 was dramatically enhanced in cells expressing both STRA6 and LRAT as compared to cells expressing only STRA6 (Figure 1B). The observation that neither retinyl esters (RE) nor all-*trans*-retinol were detected in STRA6-expressing cells indicated a key role of LRAT for efficient retinol uptake into target cells. To quantify differences in retinol uptake, we determined the kinetics of this process by incubating STRA6/LRAT- and LRAT-expressing cells with holo-RBP4. This experiment revealed an up to 8-fold higher retinol uptake by cells expressing both STRA6 and LRAT (Figure 1C). The uptake and esterification of retinol followed hyperbolic kinetics and reached saturation after 25 hr of incubation.

STRA6 Mediates Bidirectional Transport of Retinol

We next addressed the question of whether STRA6 also mediates the release of retinol from cells by adding all-*trans*-retinol (10 μM) to the culture medium to preload STRA6/LRAT- and LRAT-expressing cells with RE. Both cell lines produced comparable amounts of RE upon incubation with all-*trans*-retinol (see Figure S1 available online). Cells then were washed with PBS buffer to remove all-*trans*-retinol. Subsequently, fresh medium containing 8 μM of apo-RBP4 was added. After 16 hr incubation, we analyzed the retinoid composition of the medium by HPLC. Indeed, the quantity of all-*trans*-retinol was greatly increased in

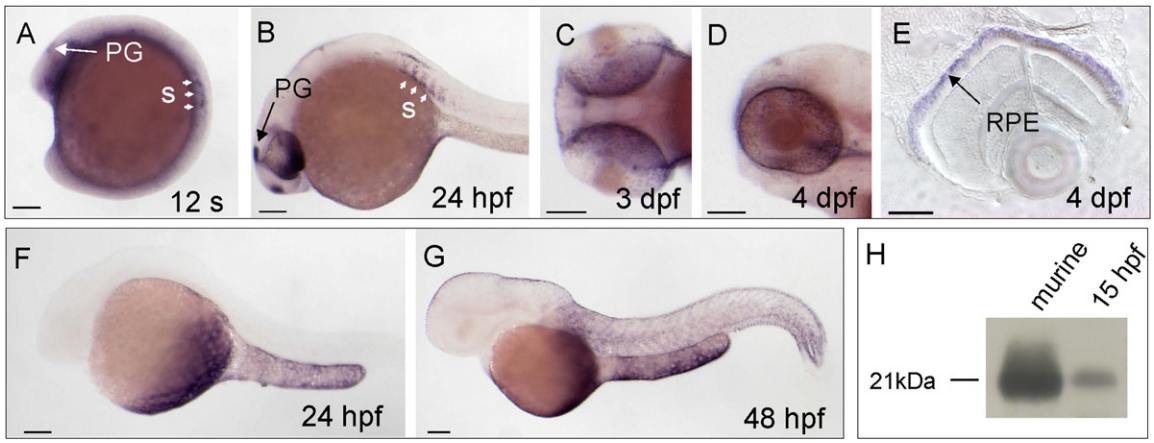

Figure 2. *stra6* and *rbp4* mRNA Expression during Zebrafish Development Analyzed by Whole-Mount In Situ Hybridization

(A) At the 12-somite stage, *stra6* mRNA (blue) is expressed in the yolk syncytium and in mesendodermal cells in the head and trunk region. Staining is also detectable in the eye anlage, the pineal gland (PG), and anterior somites (arrowheads).

(B) At 24 hours postfertilization (hpf), staining for *stra6* (blue) is seen in the developing eyes, the anterior midbrain, the pineal gland (PG), and anterior somites (arrowheads).

(C and D) At the 3 and 4 days postfertilization (dpf) larval stages, *stra6* mRNA is expressed in the eyes and the pineal gland.

(E) Cross-section through an eye of a 4 dpf larva shows *stra6* expression (blue) in the retinal pigment epithelium (RPE).

(F and G) *rbp4* mRNA expression (blue) in a 24 hpf (F) and 48 hpf (G) embryo. Staining patterns reveal that *rbp4* is expressed in the yolk syncytial layer.

(H) Immunoblot analysis for Rbp4 expression in 15 hpf embryos. Murine plasma (0.1 μl) was used as a control.

Scale bars = 100 μm. Anterior is to the left in all pictures.

the medium of cells expressing both STRA6 and LRAT as compared to that of cells expressing LRAT alone (Figure 1D). Thus, STRA6 appears to function as a channel or transporter that mediates bidirectional transport of retinol in partnership with RBP4.

Uptake of RA Is Not STRA6 Dependent

Because STRA6 deficiency causes multisystem developmental malformations of various organs, STRA6 has been suggested to play a role in the uptake of RA, the biologically active vitamin A derivative during development (Golzio et al., 2007). To test this hypothesis in the cell culture system, we loaded apo-RBP4 with RA and incubated the holo-RA-RBP4 complex with cells expressing STRA6 and LRAT for 16 hr. Even though we found RA bound to RBP4 (Figure 1E, inset), RA did not accumulate in STRA6/LRAT-expressing cells. In contrast, RA not bound to RBP4 was efficiently taken up by these cells (Figure 1E), and various RA stereoisomers became detectable in these cells. Thus, we found no evidence in cell culture that STRA6 can mediate RA uptake from a holo-RA-RBP4 complex.

Expression of *rbp4* and *stra6* in Zebrafish Development

We next used the zebrafish to analyze Stra6 function in an animal model. An *rbp4* homologous gene was recently identified in this teleost (Tingaud-Sequeira et al., 2006), and a putative zebrafish *stra6* homologous gene has also been reported in the Ensembl database (www.ensembl.org/Danio_rerio/index.html). Both *rbp4* and *stra6* genes appear to be present as single copies in the zebrafish (www.ensembl.org/Danio_rerio/index.html). We cloned the corresponding cDNAs by RT-PCR and verified their sequences after full-length cloning. The predicted amino acid sequences of zebrafish Stra6 and Rbp4 shared an overall identity with their murine and human counterparts (Figure S2). We then analyzed *stra6* and *rbp4* mRNA expression patterns with antisense RNA probes by whole-mount in situ hybridization (WISH) (Figure 2). Zebrafish *rbp4* was expressed in the yolk syncytial layer, starting with segmentation stages and persisting in these cells as development proceeded (Figures 2F and 2G). We also verified Rbp4 expression at the protein level by immunoblot analysis with an antiserum raised against human RBP4 (Figure 2H). Expression of *stra6* was detectable in the yolk syncytium and in mesendodermal cells in the head and trunk region during early somitogenesis stages (Figure 2A). At 24 hours postfertilization (hpf), expression of *stra6* appeared to be maintained in some of these tissues, albeit at a decreased level (data not shown). Moreover, staining for *stra6* mRNA became detectable in anterior somites (Figures 2A and 2B), which have been shown to contribute to RA production for hindbrain development (Begemann et al., 2001). Additionally, *stra6* was expressed in the eye anlage and the pineal gland at this embryonic stage (Figures 2A and 2B). The pineal gland is a light-sensitive endocrine organ that requires vitamin A for the production of a pineal-specific rhodopsin (Ziv and Gothilf, 2006). At later developmental stages, *stra6* expression became restricted to the developing eyes and pineal gland (Figures 2C and 2D) and was not detectable in other tissues. Cross-sections through the eyes of 4 days postfertilization (dpf) larvae revealed that *stra6* mRNA was expressed in the retinal pigment epithelium (RPE) (Figure 2E).

Stra6 Knockdown Causes Embryonic Malformations

We used an antisense morpholino oligonucleotide (MO) approach (Nasevicius and Ekker, 2000) to perform a Stra6 loss-of-function study. We designed two nonoverlapping MOs directed against the 5′ region of the *stra6* mRNA, covering bases −27 to −3 (MO1) and −1 to +24 (MO2). Additionally, we

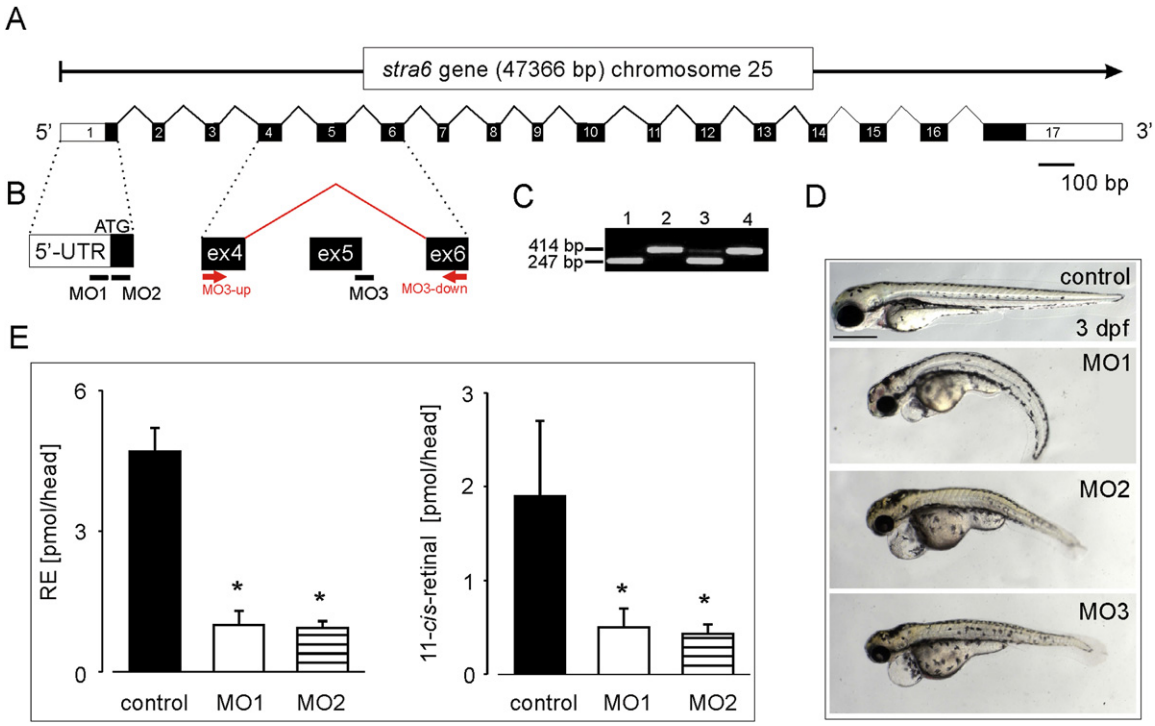

Figure 3. Targeted Gene Knockdown of Stra6 Causes Embryonic Abnormalities and Vitamin A Deficiency in Developing Eyes

(A) Schematic structure of the zebrafish *stra6* gene. White boxes indicate the 5′- and 3′-primed untranslated regions (UTRs), and black boxes represent the coding regions of the *stra6* mRNA.

(B) Morpholino oligonucleotide (MO) binding sites directed against the *stra6* mRNA. Binding of MO1 and MO2 blocks translation of the *stra6* mRNA. For the deletion of exon 5, MO3 is targeted to the exon 5 splice donor site of the *stra6* pre-mRNA.

(C) RT-PCR analysis with exon 5-spanning primers MO3-up and MO3-down (see [B]) confirms the deletion of exon 5 in MO3-treated morphants. Lane 1, MO3-treated embryo with developmental defects (see [D]); lane 2, control embryo; lane 3, MO3-treated embryo without severe developmental defects; lane 4, control embryo.

(D) Photographs of 3 dpf control and characteristic *stra6* morphant larvae injected with MO1, MO2, and MO3, respectively.

(E) Retinyl esters (RE) and 11-*cis*-retinal levels in the heads of 4 dpf MO1 and MO2 morphants as compared to control larvae. Values represent the mean ± SD of three independent experiments. *$p < 0.005$ versus control by Student's t test.

used a splice donor site MO (MO3) to delete exon 5 of the *stra6* mRNA (Figures 3A and 3B). The deletion of this exon resulted in a frameshift in the coding region of the corresponding mRNA, thereby disrupting the C-terminal part of the encoded Stra6 protein. After injection of each of these MOs into fertilized oocytes, we determined microscopically whether Stra6 deficiency caused developmental abnormalities. Morphants injected with any of the three MOs developed microphthalmia, had a curved body axis, and showed heart edema (Figure 3D). This phenotype was uniformly present (98%) in MO1- and MO2-treated embryos but was less frequent (~20%) in MO3-treated embryos. RT-PCR analysis confirmed the deletion of exon 5 in the *stra6* mRNA isolated from 2 dpf MO3-treated morphants with malformations, whereas some wild-type *stra6* mRNA was still detectable in MO3 morphants without severe malformations (Figure 3C). To confirm Stra6 deficiency in morphants treated with MO1 and MO2, we determined ocular retinoid levels in 4 dpf larvae that should have developed functional photoreceptors at this stage (Easter and Nicola, 1996). HPLC revealed that total head retinoid levels were significantly reduced in these morphants (Figure 3E). RE was the most abundant vitamin A derivative, consistent with the expression of eye-specific Lrat in the RPE at this developmental time point (Isken et al., 2007). 11-*cis*-retinal, the chromophore of visual pigments, also was detectable but significantly reduced in MO1 and MO2 morphant larvae (Figure 3E). Thus, a targeted knockdown of Stra6 caused both vitamin A deficiency in larval eyes and severe embryonic malformations.

stra6 Morphants Develop Severe Embryonic Defects

We next analyzed malformations in Stra6-deficient embryos in further morphological detail. Cross-sections through the eyes of 4 dpf larvae confirmed microphthalmia but revealed distinct retinal cell layers with normal stratification (Figures 4A and 4B). Furthermore, morphants displayed cardiac edema along with dysmorphic heart chambers (Figures 4C–4E). To better visualize pathological alterations of the heart, we injected MO2 into a fish strain that expresses enhanced green fluorescent protein (EGFP) under control of the *fli1* promoter in all vasculature and the heart (Lawson and Weinstein, 2002). Confocal imaging revealed that the morphants' hearts were not looped and that their atria were dilated like a balloon (Figures 4F and 4G). In vivo observations indicated that cardiac contractions were still detectable in Stra6-deficient embryos (n = 100). However, in the morphants with the most severe cardiac edema (~30%) (Figure 4E), blood

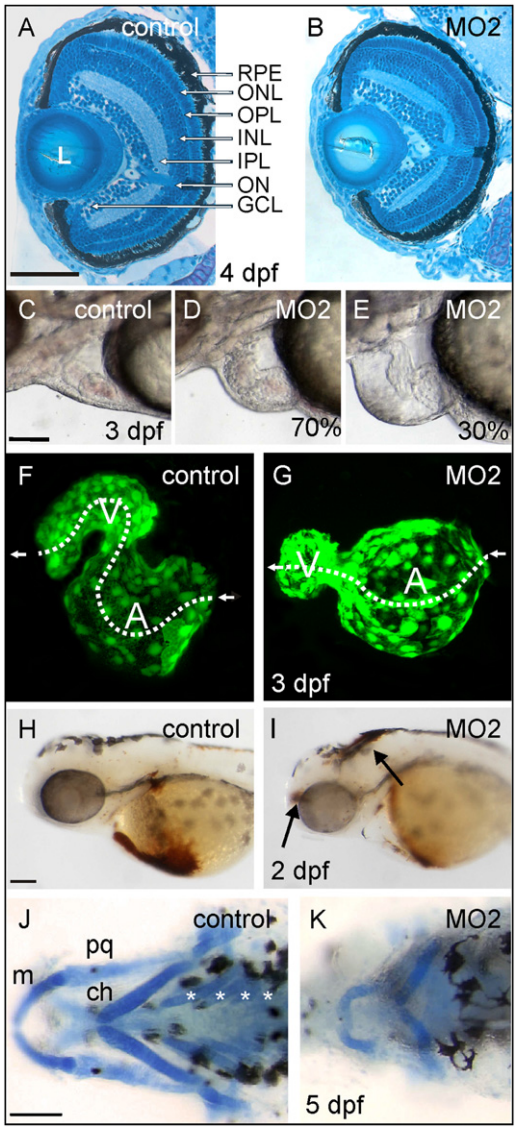

Figure 4. Stra6 Deficiency Causes Multisystemic Malformations in Zebrafish

(A and B) Cross-sections through the eye of 4 dpf control (A) and MO2 morphant (B) larvae. The *stra6* morphant eye is smaller but shows regular stratification of distinct retinal layers. L, lens; RPE, retinal pigment epithelium; ONL, outer nuclear layer; OPL, outer plexiform layer; INL, inner nuclear layer; IPL, inner plexiform layer; ON, optic nerve; GCL, ganglion cell layer.

(C–E) Close-up views of the pericardial region of control (C) and MO2-treated morphants (D and E). Characteristics of the heart shown in (D) represent 70% of the morphants; characteristics of the heart shown in (E) represent 30% of the morphants (n = 100). Note the absence of red blood cells in the heart due to a disrupted circulation in (E).

(F and G) Three-dimensional view of the heart of 3 dpf control (F) and MO2-treated (G) *TG(fli1:EGFP)*^{Y1} embryos. Blood flow is indicated by dashed lines. The ventricle (V) is on the left, and the atrium (A) is on the right.

(H and I) Control (H) and 2 dpf MO2-treated (I) embryos with the heart phenotype shown in (E) stained for hemoglobin. In controls, staining for erythrocytes was primarily detectable in the heart and afferent vessels over the yolk. In morphants, hemoglobin was greatly reduced in the heart and afferent vessels, but red blood cell extravasations were visible in the head (see arrows).

(J and K) Alcian blue staining of cartilage of the craniofacial skeleton of 5 dpf control (J) and MO2-treated morphant (K) larvae. The Meckel's cartilage (m), palatoquadrates (pq), and ceratohyales (ch) were deformed and staining of ceratobranchials (asterisks) was highly reduced in Stra6 deficiency.

Animals were raised in PTU-free water. Anterior is to the left in all pictures. Scale bars = 100 μm in (A)–(E) and (H)–(K).

did not circulate and staining for hemoglobin revealed extravasated red blood cells in the head (Figures 4H and 4I). Since morphants also exhibited an altered morphology of the craniofacial skeleton, we stained cartilage with Alcian blue (Figures 4J and 4K). The first and second arches were malformed, and the branchial arches were absent (Figure 4K). Thus, Stra6-deficient zebrafish embryos develop multisystemic malformations similar to those described for humans suffering from Matthew-Wood syndrome (Golzio et al., 2007; Pasutto et al., 2007).

Stra6 Deficiency Causes RA Excess in Several Embryonic Tissues

As evidenced by many studies, RA deficiency causes patterning defects of the neural tube, somites, heart, and eyes in both zebrafish and mice (Begemann et al., 2001; Grandel et al., 2002; Hamade et al., 2006; Keegan et al., 2005; Niederreither et al., 1999). Thus, an explanation for the pleiotropic malformations in the morphants could be a role of Stra6 in acquiring yolk vitamin A needed for retinoid signaling. However, consistent with the initiation of *stra6* mRNA expression at somitogenesis, we found normal patterning of the hindbrain and somites by double WISH staining for *krox20/myoD* markers in the morphants (Figures 5A and 5B). Analysis of *pax6.1* as an eye marker revealed that the presumptive retina was slightly smaller than normal in 21-somite embryos (Figures 5C and 5D). However, there was no loss of ventral parts of the retina, a characteristic described for RA-deficient zebrafish embryos (Hyatt et al., 1996; Marsh-Armstrong et al., 1994).

We next analyzed *cyp26a1* mRNA levels. This retinoid hydroxylase catabolizes RA to polar metabolites, and its mRNA levels are upregulated in an RA-dependent manner (Abu-Abed et al., 2001; Emoto et al., 2005). In 23-somite embryos, we found no difference in *cyp26a1* mRNA expression between morphants and controls (Figures 5E and 5F). At 31 hpf, *cyp26a1* mRNA expression was reduced but not absent in the developing eyes of morphants (Figures 5G and 5H). Interestingly, *cyp26a1* expression outside of the eyes was enhanced, e.g., in the pericardial region (Figures 5G and 5H) and in caudal parts of MO2 morphant embryos (Figures 5I and 5J). Thus, targeted knockdown of Stra6 does not cause embryonic RA deficiency at early developmental stages but rather results in excess RA production in several tissues as development proceeds.

Embryonic Defects Are Alleviated by Reducing RBP4 Levels

Based on the observation of elevated *cyp26a1* mRNA expression in the morphants, we speculated that holo-Rbp4 in the absence of Stra6 might cause local nonspecific RA excess, e.g., in the developing heart. Thus, we tried to prevent developmental abnormalities by reducing Rbp4 levels pharmacologically with the tyrosinase inhibitor 1-phenyl-2-thiourea (PTU) as well as by blocking *rbp4* mRNA translation with an *rbp4*-MO covering −6 to +19 of the *rbp4* mRNA. PTU inhibits pigmentation in zebrafish and also has been shown to downregulate *rbp4* mRNA

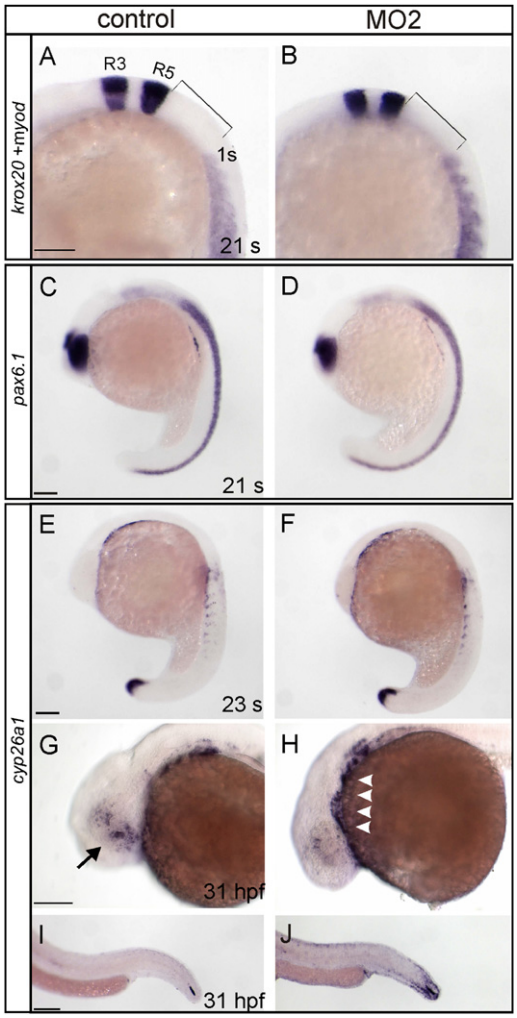

Figure 5. Comparison of Marker Gene Expression between Control and *stra6* Morphant Embryos

Marker genes and developmental stages of the embryos shown are indicated. Control embryo is shown at the left; *stra6* morphant embryo is shown at the right. Animals were raised in PTU-free water.

(A and B) Double staining for *krox20* and *myoD* reveals normal patterning of the hindbrain rhombomeres and somites. Additionally, the distance between rhombomere 5 (R5) and the first somite (1 s) is comparable between control and morphant embryos.

(C and D) Staining for *pax6.1* (blue) at the 21-somite stage shows that the presumptive retina is smaller in *stra6* morphants than in controls but that patterns of *pax6.1* mRNA expression are comparable along the anteroposterior axis.

(E–J) Staining for *cyp26a1* mRNA expression.

(E and F) *cyp26a1* mRNA expression was indistinguishable between controls and MO2 morphants at the 23-somite stage.

(G–J) *cyp26a1* mRNA expression was reduced in the developing eye of MO2-treated morphants as compared to controls (arrow in [G]), but deeper staining appeared in the pericardial region (arrowheads in [H]) and in caudal parts of the morphant embryo (J) as compared to the control (I).

Scale bars = 100 μm. Anterior is to the left in all pictures.

expression at larval stages (Tingaud-Sequeira et al., 2006). To confirm that PTU reduces Rbp4 levels during embryonic development, we performed WISH and immunoblot analyses. Both *rbp4* mRNA expression and Rbp4 protein levels were decreased in the presence of 200 μM PTU in 24 hpf control and MO2 morphant embryos (Figures 6A and 6C). We also confirmed the reduction of Rbp4 levels by immunoblot analysis in *rbp4*-MO-treated embryos (Figure 6C). To show that reduced embryonic Rbp4 levels led to a diminished mobilization of yolk vitamin A, we determined retinoid levels of 4 dpf larvae. When animals were raised in the presence of PTU, retinoid content was significantly reduced in the larval eyes but significantly increased in the trunk (Figure 6B). Similarly, *rbp4* morphants showed significantly reduced levels of retinoids in the eyes and significantly increased retinoid levels in the trunk (Figure 6B). Importantly, both PTU and *rbp4*-MO treatments caused no obvious developmental abnormalities (Figures 6D and 6E), such as microphthalmia and cardiac defects, as we had found in Stra6-deficient embryos.

To determine whether a reduction of Rbp4 levels could prevent developmental abnormalities in MO2 morphants, we microscopically analyzed morphant larvae raised in the presence and absence of this compound (n = 170 for each condition). When MO2 and PTU treatments were combined, visible developmental malformations were prevented in 73% of morphants (Figure 6D). In contrast, virtually all MO2-treated embryos raised in the absence of PTU showed cardiac edema and morphologically altered heart chambers (Figure 6D). Coinjection of both MO2 and *rbp4*-MO also prevented developmental impairment in 77% of the embryos, whereas all siblings injected with only MO2 developed the characteristic abnormalities (Figure 6E). Thus, reduction of embryonic Rbp4 levels either by pharmacological treatment via PTU or by *rbp4*-MO treatment can reduce the high fatality observed in Stra6-deficient zebrafish embryos.

DISCUSSION

Vitamin A is required throughout the vertebrate life cycle, e.g., for vision and cell proliferation and differentiation. All-*trans*-retinol-bound RBP4 (holo-RBP4) is the most abundant retinoid derivative present in the circulation of humans and most vertebrates. In humans, inherited blood retinol deficiency has been described in a family with compound heterozygous missense mutations in *RBP4*. Two affected subjects had reduced visual acuity, night blindness, and mild ocular fundus atrophy (Biesalski et al., 1999). Consistent with these defects, RBP4-deficient mice appear phenotypically normal except for a visual impairment early in life (Quadro et al., 1999). Thus, it is generally accepted that RBP4 is required to maintain ocular vitamin A-dependent processes of vision but is not essential for embryonic RA production. Recently, STRA6 has been suggested to act as a holo-RBP4 receptor that facilitates uptake of vitamin A into target tissues (Kawaguchi et al., 2007). Hence, it was surprising that STRA6 deficiency causes human Matthew-Wood syndrome with multisystem malformations related to impaired RA signaling (Golzio et al., 2007; Pasutto et al., 2007). This finding conflicts with the proposed role of STRA6 as the long-sought holo-RBP4 receptor and suggests an additional unknown role for this membrane protein.

STRA6-Dependent Vitamin A Uptake Depends on LRAT

To address the biochemical basis of STRA6 deficiency, we established both a cell culture and an animal model. We cloned

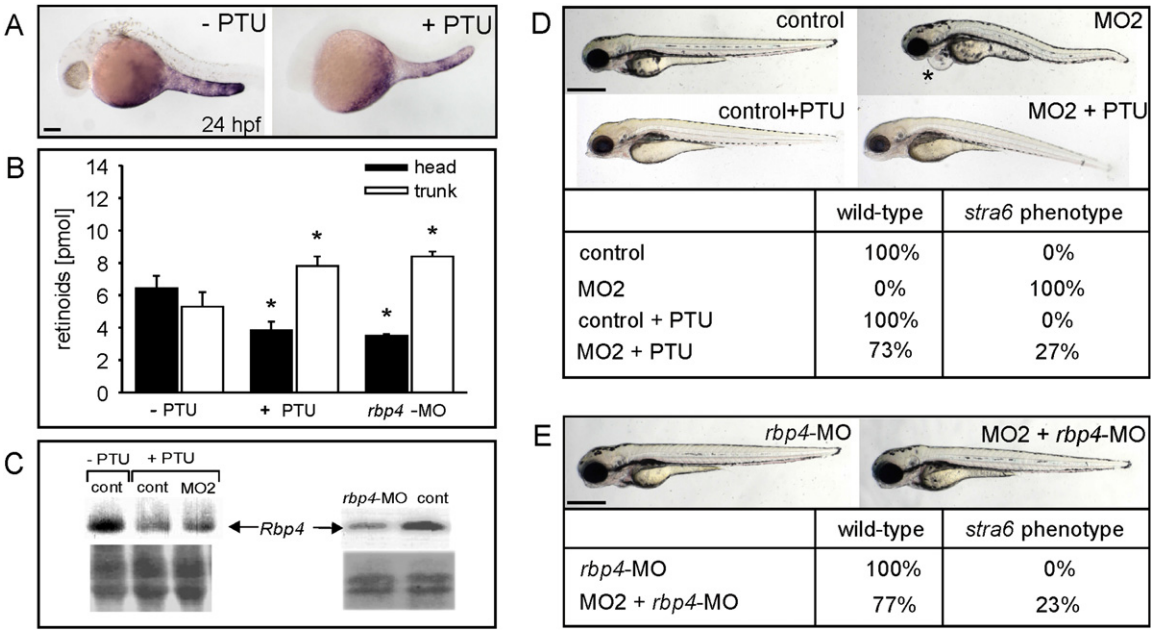

	wild-type	*stra6* phenotype
control	100%	0%
MO2	0%	100%
control + PTU	100%	0%
MO2 + PTU	73%	27%

	wild-type	*stra6* phenotype
rbp4-MO	100%	0%
MO2 + *rbp4*-MO	77%	23%

Figure 6. PTU and *rbp4*-MO Treatments Prevent Developmental Abnormalities in *stra6* Morphants

(A) *rbp4* mRNA expression (blue) was reduced in PTU-treated embryos.

(B) Retinoids (retinaldehyde and RE) of the head and trunk of 4 dpf control and PTU- and *rbp4*-MO-treated larvae. Values represent the means ± SD of three independent experiments. *$p < 0.02$ versus control by Student's t test.

(C) Immunoblot analysis of Rbp4 levels in 24 hpf embryos treated with PTU, PTU and MO2 (left), and *rbp4*-MO (right) as compared to respective controls. Ponceau S red-stained membranes are shown as a loading control (lower panel).

(D) *stra6* morphants and controls were raised in the presence and absence of PTU (n = 170 each). Representative photographs of 3 dpf larvae are shown. PTU treatment prevented developmental abnormalities in 73% of the *stra6* morphants. In the absence of PTU, all *stra6* morphants displayed cardiac edema (asterisk).

(E) Larvae raised from oocytes either injected with *rbp4*-MO or coinjected with *rbp4*-MO and MO2. These morphant larvae were raised in the absence of PTU. *rbp4* morphant larvae showed no developmental abnormalities (n = 120). Coinjection of *rbp4*-MO and MO2 largely prevented developmental abnormalities in 77% of the compound morphants (n = 120).

Scale bar = 100 μM in (A) and 500 μm in (D) and (E). Anterior is to the left in all pictures.

zebrafish *rbp4* and *stra6* genes and showed that their expression was initiated at segmentation stages, shortly before functional circulation developed. At later larval stages, *stra6* mRNA expression was restricted to the RPE of the eyes, indicating that the organism acquires vitamin A from holo-Rbp4 to support vision. Indeed, targeted knockdown of Stra6 caused biochemically detectable vitamin A deficiency of the larval eyes, thereby verifying the proposed function of STRA6 as a retinoid channel/transporter in an in vivo animal model.

Our cell culture studies revealed that only those cells expressing both STRA6 and LRAT accumulated significant amounts of vitamin A. Our finding that cells expressing STRA6 lacked retinoids suggests the existence of an intracellular, low-abundance acceptor for vitamin A. We provide several lines of evidence that LRAT acts as this acceptor. In cell culture, the flow of vitamin A between extra- and intracellular compartments is driven by metabolic conversion via LRAT toward cellular accumulation of RE. This idea is further supported by our findings in the zebrafish model. Both Lrat and Stra6 are expressed in the RPE, and RE accumulates in developing zebrafish eyes. Furthermore, *lrat* expression, like that of *stra6*, is already initiated early in development in the pineal gland at 24 hpf and in the eyes at 56 hpf (Figure 2B; Isken et al., 2007). This requirement of LRAT for STRA6-dependent vitamin A accumulation also is manifest in a mammalian model: *Lrat* null mice are selectively vitamin A deficient in the eyes and liver (Batten et al., 2004). Thus, we propose that RBP4, STRA6, and LRAT act sequentially in vitamin A uptake by target tissues. The fact that mammals including humans produce RE in various tissues, e.g., the liver, lung, and eyes, may provide an explanation for the more widespread expression of STRA6 and LRAT in mammals (Batten et al., 2004; Kawaguchi et al., 2007) as compared to zebrafish (Figure 2; Isken et al., 2007). Additionally, we found that the STRA6 retinoid channel transports retinol bidirectionally in an RBP4-dependent manner, most probably facilitating attainment of steady-state concentrations of vitamin A between intracellular and extracellular pools. Such a STRA6-dependent homeostatic regulation of retinoid levels between extra- and intracellular compartments may play a more important role in mammalian embryos needing a continuous maternal supply of vitamin A than in zebrafish embryos that rapidly consume yolk vitamin A to establish vision.

STRA6 Is Essential to Maintain Embryonic RA Homeostasis

Our cell culture analyses exclude a role for STRA6 in acquiring RA, the developmentally active form of vitamin A, as has been recently suggested by others (Golzio et al., 2007). We found no evidence that RBP4-bound RA is accumulated by STRA6-expressing cells. This suggests high substrate specificity for STRA6 or a requirement for an intracellular RA-binding protein

that interacts with STRA6. Our analyses of the zebrafish model revealed that Stra6 deficiency causes, in addition to retinoid deficiency of the eyes, developmental abnormalities that include ocular, cardiac, and craniofacial malformations as described for STRA6-deficient patients who suffer from Matthew-Wood syndrome (Golzio et al., 2007; Pasutto et al., 2007). Microphthalmia can be related to RA deficiency (Marsh-Armstrong et al., 1994), but in contrast to RA-deficient zebrafish embryos (Biehlmaier et al., 2005; Lampert et al., 2003), there was normal overall stratification of the retinal layers in Stra6-deficient embryos. Additionally, we observed no loss of ventral parts of the retina as has been described in RA-deficient zebrafish embryos (Hyatt et al., 1996). In zebrafish, RA-dependent patterning processes of the developing eyes depend largely on β-carotene as the RA precursor (Lampert et al., 2003). Thus, this process does not essentially require retinol delivered by holo-Rbp4 for RA production. Consistent with the absence of severe developmental eye defects, β-carotene together with circulating RE also has been suggested to prevent ocular defects in RBP4 deficiency in mammals, including humans (Paik et al., 2004). Importantly, RA is required for optic cup specification later in development in mammals (Molotkov et al., 2006). Accordingly, lack of RA production in developing murine eyes does not cause severe microphthalmia (clinical anophthalmia) (Molotkov et al., 2006) as has been described for patients suffering from Matthew-Wood syndrome (Golzio et al., 2007; Pasutto et al., 2007). Thus, as evidenced here for zebrafish, secondary effects, most probably RA excess in surrounding tissues, cause microphthalmia in Stra6 deficiency. Cardiac and craniofacial abnormalities in Stra6-deficient zebrafish embryos could be also ascribed to embryonic RA excess rather than RA deficiency. This outcome was suggested by marker gene analysis showing elevated *cyp26a1* expression in the developing heart together with the absence of *stra6* expression in this organ. Thus, we speculated that these developmental abnormalities are caused by circulating holo-Rbp4 that cannot be cleared from the circulation in Stra6 deficiency. To reduce embryonic Rbp4 levels, we used PTU, a substance that inhibits pigmentation but also reduces *rbp4* expression (Figure 6; Tingaud-Sequeira et al., 2006). Additionally, we designed an *rbp4*-MO to block *rbp4* mRNA translation. Both treatments reduced Rbp4 protein levels and the mobilization of yolk vitamin A. More importantly, they largely prevented developmental abnormalities in the Stra6-deficient morphants. Thus, we conclude that in Stra6 deficiency, Rbp4-bound vitamin A, which is not cleared from the circulation, provokes developmental abnormalities. This finding can be well extrapolated to the mammalian situation and provides a ready explanation for the biochemical basis of the dramatically different consequences of RBP4 and STRA6 deficiency in patients.

In summary, our study validates and extends the work of Kawaguchi and colleagues (2007). We show in an animal model that Stra6 is the long-sought holo-Rbp4 receptor. In cell culture, we demonstrate that the STRA6 retinoid channel transports retinol bidirectionally in an RBP4-dependent manner. In this process, the net flow of vitamin A between extra- and intracellular compartments is driven by metabolic conversion via LRAT to support RE production. Furthermore, we provide evidence that in Stra6 deficiency, Rbp4-bound vitamin A, which is not cleared from the circulation, leads to developmental abnormalities. Dysfunctions of STRA6 and RBP4 are related to human diseases as diverse as Matthew-Wood syndrome (Pasutto et al., 2007) and type 2 diabetes (Yang et al., 2005). Thus, the generality of our findings in cell culture and zebrafish as presented here requires further testing in mammalian models such as *Stra6* mutant and *Stra6/Rbp4* double-mutant mice.

EXPERIMENTAL PROCEDURES

Stable Transduction of the NIH 3T3 Cell Line

Full-length human *STRA6* and *LRAT* clones were purchased from the American Type Culture Collection. To construct retroviral expression vectors, *STRA6* and *LRAT* cDNAs were amplified by PCR, and EcoRI and NotI sites were introduced at the ends of the coding sequence using the primers 5′-GCAGATGAATTCACC ATGTCGTCCCAGCCAGCAGG-3′ and 5′-CGTCTAGCGGCCGCTCAGGGCT GGGCACCATTGG-3′ for *STRA6* and 5′-GAGGTGAATTCAGCTACTCAGGGA TGAAGAACCCCATGCTG-3′ and 5′-ACTGACGCGGCCGCATGAAGTTAGCC AGCCATCCATAG-3′ for *LRAT*. These constructs were cloned into pMXs-IG or pMXs-IP retroviral vectors provided by T. Kitamura (University of Tokyo) (Kitamura et al., 2003). Inserts were sequenced and confirmed to be identical to *STRA6* and *LRAT* reference sequences deposited in the Ensembl database (www.ensembl.org). Stable transfectants of NIH 3T3 fibroblasts were generated using standard methods.

Immunohistochemistry

For cellular STRA6 detection, STRA6 was tagged at its C terminus with a 15-amino acid epitope (SATASKTETSQVAPA) corresponding to the ROS targeting sequence found in the C terminus of mouse rhodopsin (1D4). The 1D4 sequence was introduced by PCR using the primer 5′-TTCTAGCGGCCGC TCAGGCAGGCGCCACCTGGCTGGTCTCTGTGGGCTGGGCACCATTGG-3′. Localization of 1D4-tagged STRA6 was performed by fixing NIH 3T3 cells expressing STRA6-1D4 with 4% paraformaldehyde in PBS for 10 min. Cells were washed three times with PBST (PBS with 0.1% Triton X-100) and incubated in 1.5% normal goat serum in PBST for 15 min at room temperature to block nonspecific binding. Cells then were incubated sequentially with anti-1D4-tagged monoclonal antibody followed by rabbit anti-calreticulin polyclonal antibody. Cells were rinsed in PBST three times and stained with Cy5-conjugated goat anti-mouse IgG and Cy3-conjugated goat anti-rabbit IgG for detection of calreticulin. Cells were mounted in 2% 1,4-diazabicyclo[2,2,2] octane in 90% glycerol to retard photobleaching and imaged with a Leica TCS SP2 confocal/multiphoton microscope equipped with a titanium/sapphire laser (Chameleon-XR, Coherent, Inc.).

Expression and Purification of Human RBP4

Human *RBP4* cDNA cloned into a pET3a expression vector was a kind gift from J.W. Kelly (The Scripps Research Institute). The procedure used for RBP4 expression in *E. coli* was based on previously published methodology with slight modifications (Xie et al., 1998). Briefly, RBP4 was expressed in BL21 cells according to a standard protocol. These bacterial cells were harvested and lysed by osmotic shock (Burger et al., 1993). Insoluble material was pelleted, washed three times with 20 mM Tris-HCl (pH 8.0), and solubilized in 7 M guanidine hydrochloride and 10 mM DTT. Buffer (25 mM Tris-HCl [pH 8.8]) was added to dilute the guanidine hydrochloride concentration to 5.0 M. After overnight incubation, insoluble material was removed by ultracentrifugation (120,000 × g, 1 hr, 4°C), and the collected supernatant was used for the RBP4 refolding procedure. RBP4 was refolded by dropwise addition of solubilized material to a mixture containing 25 mM Tris-HCl (pH 8.8), 0.3 mM cystine, 3.0 mM cysteine, 1 mM EDTA, and 1 mM retinol delivered in ethanol at 4°C. The reaction was continued for 5 hr at 4°C with vigorous mixing. The precipitate was removed by ultracentrifugation (120,000 × g, 1 hr, 4°C), and the supernatant was dialyzed against 10 mM Tris-HCl (pH 8.0) at 4°C overnight, filtered, and loaded on a DE53 ion exchange chromatography column. Refolded holo-RBP4 was eluted by a linear gradient of NaCl (0–300 mM) in 10 mM Tris-HCl (pH 8.0). Collected fractions were examined by SDS-PAGE and UV-visible spectroscopy. Fractions containing RBP4 with an absorbance ratio of 0.9 or higher at 280/330 nm were pooled together, concentrated to 6 mg/ml with a ten-tube Amicon Centriprep concentrator, and stored at −80°C.

Loading of RBP4 with RA

All-*trans*-retinol was extracted from holo-RBP4 with diethyl ether as described previously (Cogan et al., 1976). The efficiency of retinol release was monitored by recording spectra of both the aqueous and organic phases. A solution of apo-RBP4 (2 mg/ml) in 20 mM Tris-HCl (pH 8.0) was incubated with 1 mM RA delivered in ethanol in the presence of glycerol (10%) for 2 hr at 4°C. The sample was diluted with 20 mM Tris-HCl (pH 8.0), centrifuged, and repurified on a Uno Q ion exchange column (Bio-Rad). The presence of RBP4-bound RA was confirmed by its absorbance spectrum after purification by HPLC.

Retinoid Uptake Assays

Twenty hours prior to the experiment, NIH 3T3 cells expressing LRAT, STRA6, or STRA6/LRAT were cultured in six-well culture plates at a density of 1×10^6 cells per well. After growth medium removal, cells were washed with PBS, and serum-free medium containing holo-RBP4 was added. After incubation, cells were washed with PBS twice, harvested, and extracted with 1 volume of methanol followed by 2 volumes of hexane. The organic phase was collected, dried down in a SpeedVac, and redissolved in 250 μl of hexane, and the composition of retinoids was analyzed by normal-phase HPLC on a Hewlett Packard 1100 series HPLC system equipped with a diode array detector. Retinyl esters were separated using an Agilent SI column (4.6 × 250 mm, 5 μm) and a stepped gradient of ethyl acetate in hexane (0.5% for 15 min and 20% up to 30 min at flow rate of 1.4 ml/min). The extraction procedure and reverse-phase HPLC conditions used for RA were described previously (Moise et al., 2005).

Retinol Release Assays

Prior to the experiment, cells expressing LRAT or STRA6/LRAT were incubated with 10 μM all-*trans*-retinol in growth medium for 16 hr. Cells were then washed with PBS, and fresh medium containing 8 μM apo-RBP4 was added. After 16 hr incubation, the medium was collected and retinoid composition was analyzed by HPLC under the conditions described above.

Cloning of Zebrafish *stra6* and *rbp4*

We searched the Ensembl zebrafish database (www.ensembl.org/Danio_rerio/index.html) and found a cDNA sequence (GenBank accession number BC076188) encoding a protein with high overall amino acid sequence identity to mouse and human STRA6. For cloning, we performed RT-PCR with whole RNA preparations from 3 dpf larvae and the oligonucleotide primers *stra6*-up 5′-ATGAGTGCTGAAACTGTGAATAACT-3′ and *stra6*-down 5′-TCAGTTGCTGGCAGCGGCGCT-3′. *stra6* cDNA was cloned into the vector pCRII-TOPO (Invitrogen) and verified by sequencing. Zebrafish *rbp4* cDNA (GenBank accession number AJ236884) was obtained by RT-PCR using the primers *rbp4*-up 5′-ATGTTAAGGCTCTGTATAGCA-3′ and *rbp4*-down 5′-TTAGGCAGCCTCACAGAAAC-3′.

Fish Maintenance and Strains

Zebrafish (strain AB/TL) were bred and maintained under standard conditions at 28.5°C (Westerfield, 1994). For analyzing heart morphology, we used the *TG(fli1:EGFP)*^{Y1} strain (Lawson and Weinstein, 2002). Morphological features were used to determine the stage of the embryos in hpf or dpf (Kimmel et al., 1995). Embryos were raised in either the presence or the absence of 200 μM 1-phenyl-2-thiourea (PTU, Sigma-Aldrich) as indicated in the figure legends.

Immunoblotting

Embryos (five per lane) were homogenized and subjected to SDS-PAGE. Immunoblot analysis was performed using monoclonal antibody raised against human RBP4 (ab8609, Abcam) at a 1:500 dilution. Immunoblots were developed with the ECL system (Amersham Bioscience).

WISH and Histology

WISH was performed as described by Hauptmann and Gerster (1994). *stra6* was cloned into the vector pCRII-TOPO (Invitrogen), and an antisense RNA probe was synthesized with the T7 RNA polymerase. Additional RNA probes used for in situ hybridization experiments were *cyp26a1* (Emoto et al., 2005), *krox20* (Oxtoby and Jowett, 1993), *myoD* (Weinberg et al., 1996), *pax6.1* (Nornes et al., 1998), and *rbp4* (Tingaud-Sequeira et al., 2006). RNA probes were generated with the DIG RNA Labeling Kit (Roche Molecular Biochemicals) according to the manufacturer's protocol.

Histology of tissues and staining for cartilage was performed as described previously (Lampert et al., 2003)

Morpholino Oligonucleotide Knockdown

For targeted knockdown of Stra6 protein, the following morpholino oligonucleotides (Gene Tools, LLC) were used. For blocking *stra6* mRNA translation, we designed MO1 5′-TGCCAACCTATACAGCAAACAGAAG-3′ covering −27 to −3 and MO2 5′-GTTATTCACAGTTTCAGCACTCATG-3′ covering −1 to +24 of the *stra6* mRNA. Additionally, we used MO3 5′-TATCTATTGTAAGTTATACCTGTGG-3′ directed against the splice donor site of exon 5 of the *stra6* pre-mRNA. For blocking *rbp4* mRNA translation, we designed *rbp4*-MO 5′-CTATACAGAGCCTTAACATACTTCC-3′ covering −6 to +19 of the *rbp4* mRNA. The MOs were dissolved in 0.3× Danieau's solution (1× Danieau's solution: 5 mM HEPES [pH 7.6] containing 58 mM NaCl, 0.7 mM KCl, 0.4 mM $MgSO_4$, 0.6 mM $Ca(NO_3)_2$) to obtain a stock concentration of 1 mM (8.4 mg/ml). 8 ng MO1, 15 ng MO2, 20 ng MO3, or 20 ng *rbp4*-MO was routinely injected per oocyte. For coinjections, 15 ng MO2 and 10 ng *rbp4*-MO were used per oocyte. The injected volume was 3 nl. We used RT-PCR analysis to confirm deletion of exon 5. For this purpose, we isolated total RNA from 2 dpf morphant and control embryos (n = 20 each) with the RNeasy kit (QIAGEN) according to the manufacturer's protocol. Reverse transcription was carried out with 70 ng total RNA and SuperScript reverse transcriptase (Invitrogen). For PCR, we used Taq polymerase (Stratagene) and the primers MO3-up 5′-TTTAGACCACACGCAACACAAG-3′ and MO3-down 5′-CTCAGAGGCATTGGCTGTCTC-3′.

HPLC Analysis of Retinoids in Zebrafish Larvae

Fish were raised in darkness prior to extraction of retinoids. To determine the retinoid content of 4 dpf larval eyes and trunks, we removed the anterior part of the head, including the eyes, by hand dissection with a scalpel. HPLC analysis was carried out as described previously (Isken et al., 2007). For retinoid quantification, peak integrals were scaled with defined amounts of reference substances and quantified using 32 Karat software (Beckman Instruments). Student's t test was used for statistical analyses.

Photography

Photographs were taken of live embryos fixed in 2.5% methylcellulose/0.02% 3-aminobenzoic acid methyl ester (Sigma-Aldrich). Stained whole-mount embryos were photographed in 100% glycerol under a Leica MZ FLIII dissecting microscope with a Zeiss AxioCam. Confocal images of hearts from 3 dpf *TG(fli1:EGFP)*^{Y1} and MO2-treated 3 dpf *TG(fli1:EGFP)*^{Y1} embryos (n = 3 each) embedded in 1% low-melting agarose were taken with a Zeiss LSM 510 Meta upright confocal microscope using an Achroplan 40×/0.8 W objective. Three-dimensional pictures were constructed with Imaris 3.1 software (Bitplane AG).

SUPPLEMENTAL DATA

Supplemental Data include two figures and can be found with this article online at http://www.cellmetabolism.org/cgi/content/full/7/3/258/DC1/.

ACKNOWLEDGMENTS

We thank L. Webster, Jr. for comments on the manuscript. We are grateful to B. Weinstein (National Institute of Child Health and Human Development, NIH) for the gift of the zebrafish *TG(fli1:EGFP)*^{Y1} strain. This work was supported by a grant from the Ministry of Science and Art, Baden-Württemberg to J.v.L. and by NIH grants EY09339 and P30 EY11373 to K.P.

Received: July 13, 2007
Revised: November 21, 2007
Accepted: January 31, 2008
Published: March 4, 2008

REFERENCES

Abu-Abed, S., Dolle, P., Metzger, D., Beckett, B., Chambon, P., and Petkovich, M. (2001). The retinoic acid-metabolizing enzyme, CYP26A1, is essential for

normal hindbrain patterning, vertebral identity, and development of posterior structures. Genes Dev. *15*, 226–240.

Batten, M.L., Imanishi, Y., Maeda, T., Tu, D.C., Moise, A.R., Bronson, D., Possin, D., Van Gelder, R.N., Baehr, W., and Palczewski, K. (2004). Lecithin-retinol acyltransferase is essential for accumulation of all-trans-retinyl esters in the eye and in the liver. J. Biol. Chem. *279*, 10422–10432.

Begemann, G., Schilling, T.F., Rauch, G.J., Geisler, R., and Ingham, P.W. (2001). The zebrafish neckless mutation reveals a requirement for raldh2 in mesodermal signals that pattern the hindbrain. Development *128*, 3081–3094.

Biehlmaier, O., Lampert, J.M., von Lintig, J., and Kohler, K. (2005). Photoreceptor morphology is severely affected in the beta,beta-carotene-15,15′-oxygenase (bcox) zebrafish morphant. Eur. J. Neurosci. *21*, 59–68.

Biesalski, H.K., Frank, J., Beck, S.C., Heinrich, F., Illek, B., Reifen, R., Gollnick, H., Seeliger, M.W., Wissinger, B., and Zrenner, E. (1999). Biochemical but not clinical vitamin A deficiency results from mutations in the gene for retinol binding protein. Am. J. Clin. Nutr. *69*, 931–936.

Blaner, W.S. (2007). STRA6, a cell-surface receptor for retinol-binding protein: the plot thickens. Cell Metab. *5*, 164–166.

Blomhoff, R., Green, M.H., Berg, T., and Norum, K.R. (1990). Transport and storage of vitamin A. Science *250*, 399–404.

Bouillet, P., Sapin, V., Chazaud, C., Messaddeq, N., Decimo, D., Dolle, P., and Chambon, P. (1997). Developmental expression pattern of Stra6, a retinoic acid-responsive gene encoding a new type of membrane protein. Mech. Dev. *63*, 173–186.

Burger, A., Berendes, R., Voges, D., Huber, R., and Demange, P. (1993). A rapid and efficient purification method for recombinant annexin V for biophysical studies. FEBS Lett. *329*, 25–28.

Chambon, P. (1996). A decade of molecular biology of retinoic acid receptors. FASEB J. *10*, 940–954.

Cogan, U., Kopelman, M., Mokady, S., and Shinitzky, M. (1976). Binding affinities of retinol and related compounds to retinol binding proteins. Eur. J. Biochem. *65*, 71–78.

Easter, S.S., Jr., and Nicola, G.N. (1996). The development of vision in the zebrafish (Danio rerio). Dev. Biol. *180*, 646–663.

Emoto, Y., Wada, H., Okamoto, H., Kudo, A., and Imai, Y. (2005). Retinoic acid-metabolizing enzyme Cyp26a1 is essential for determining territories of hindbrain and spinal cord in zebrafish. Dev. Biol. *278*, 415–427.

Giguere, V., Ong, E.S., Segui, P., and Evans, R.M. (1987). Identification of a receptor for the morphogen retinoic acid. Nature *330*, 624–629.

Golzio, C., Martinovic-Bouriel, J., Thomas, S., Mougou-Zrelli, S., Grattagliano-Bessieres, B., Bonniere, M., Delahaye, S., Munnich, A., Encha-Razavi, F., Lyonnet, S., et al. (2007). Matthew-Wood syndrome is caused by truncating mutations in the retinol-binding protein receptor gene STRA6. Am. J. Hum. Genet. *80*, 1179–1187.

Grandel, H., Lun, K., Rauch, G.J., Rhinn, M., Piotrowski, T., Houart, C., Sordino, P., Kuchler, A.M., Schulte-Merker, S., Geisler, R., et al. (2002). Retinoic acid signalling in the zebrafish embryo is necessary during pre-segmentation stages to pattern the anterior-posterior axis of the CNS and to induce a pectoral fin bud. Development *129*, 2851–2865.

Hamade, A., Deries, M., Begemann, G., Bally-Cuif, L., Genet, C., Sabatier, F., Bonnieu, A., and Cousin, X. (2006). Retinoic acid activates myogenesis in vivo through Fgf8 signalling. Dev. Biol. *289*, 127–140.

Hauptmann, G., and Gerster, T. (1994). Two-color whole-mount in situ hybridization to vertebrate and Drosophila embryos. Trends Genet. *10*, 266.

Hyatt, G.A., Schmitt, E.A., Marsh-Armstrong, N., McCaffery, P., Drager, U.C., and Dowling, J.E. (1996). Retinoic acid establishes ventral retinal characteristics. Development *122*, 195–204.

Isken, A., Holzschuh, J., Lampert, J.M., Fischer, L., Oberhauser, V., Palczewski, K., and von Lintig, J. (2007). Sequestration of retinyl esters is essential for retinoid signaling in the zebrafish embryo. J. Biol. Chem. *282*, 1144–1151.

Kawaguchi, R., Yu, J., Honda, J., Hu, J., Whitelegge, J., Ping, P., Wiita, P., Bok, D., and Sun, H. (2007). A membrane receptor for retinol binding protein mediates cellular uptake of vitamin A. Science *315*, 820–825.

Keegan, B.R., Feldman, J.L., Begemann, G., Ingham, P.W., and Yelon, D. (2005). Retinoic acid signaling restricts the cardiac progenitor pool. Science *307*, 247–249.

Kimmel, C.B., Ballard, W.W., Kimmel, S.R., Ullmann, B., and Schilling, T.F. (1995). Stages of embryonic development of the zebrafish. Dev. Dyn. *203*, 253–310.

Kitamura, T., Koshino, Y., Shibata, F., Oki, T., Nakajima, H., Nosaka, T., and Kumagai, H. (2003). Retrovirus-mediated gene transfer and expression cloning: powerful tools in functional genomics. Exp. Hematol. *31*, 1007–1014.

Lampert, J.M., Holzschuh, J., Hessel, S., Driever, W., Vogt, K., and von Lintig, J. (2003). Provitamin A conversion to retinal via the beta,beta-carotene-15,15′-oxygenase (bcox) is essential for pattern formation and differentiation during zebrafish embryogenesis. Development *130*, 2173–2186.

Lawson, N.D., and Weinstein, B.M. (2002). In vivo imaging of embryonic vascular development using transgenic zebrafish. Dev. Biol. *248*, 307–318.

Mark, M., Ghyselinck, N.B., and Chambon, P. (2006). Function of retinoid nuclear receptors: lessons from genetic and pharmacological dissections of the retinoic acid signaling pathway during mouse embryogenesis. Annu. Rev. Pharmacol. Toxicol. *46*, 451–480.

Marsh-Armstrong, N., McCaffery, P., Gilbert, W., Dowling, J.E., and Drager, U.C. (1994). Retinoic acid is necessary for development of the ventral retina in zebrafish. Proc. Natl. Acad. Sci. USA *91*, 7286–7290.

Moise, A.R., Kuksa, V., Blaner, W.S., Baehr, W., and Palczewski, K. (2005). Metabolism and transactivation activity of 13,14-dihydroretinoic acid. J. Biol. Chem. *280*, 27815–27825.

Molotkov, A., Molotkova, N., and Duester, G. (2006). Retinoic acid guides eye morphogenetic movements via paracrine signaling but is unnecessary for retinal dorsoventral patterning. Development *133*, 1901–1910.

Nasevicius, A., and Ekker, S.C. (2000). Effective targeted gene 'knockdown' in zebrafish. Nat. Genet. *26*, 216–220.

Niederreither, K., Subbarayan, V., Dolle, P., and Chambon, P. (1999). Embryonic retinoic acid synthesis is essential for early mouse post-implantation development. Nat. Genet. *21*, 444–448.

Nornes, S., Clarkson, M., Mikkola, I., Pedersen, M., Bardsley, A., Martinez, J.P., Krauss, S., and Johansen, T. (1998). Zebrafish contains two pax6 genes involved in eye development. Mech. Dev. *77*, 185–196.

Oxtoby, E., and Jowett, T. (1993). Cloning of the zebrafish krox-20 gene (krx-20) and its expression during hindbrain development. Nucleic Acids Res. *21*, 1087–1095.

Paik, J., Vogel, S., Quadro, L., Piantedosi, R., Gottesman, M., Lai, K., Hamberger, L., Vieira Mde, M., and Blaner, W.S. (2004). Vitamin A: overlapping delivery pathways to tissues from the circulation. J. Nutr. *134*, 276S–280S.

Palczewski, K. (2006). G protein-coupled receptor rhodopsin. Annu. Rev. Biochem. *75*, 743–767.

Pasutto, F., Sticht, H., Hammersen, G., Gillessen-Kaesbach, G., Fitzpatrick, D.R., Nurnberg, G., Brasch, F., Schirmer-Zimmermann, H., Tolmie, J.L., Chitayat, D., et al. (2007). Mutations in STRA6 cause a broad spectrum of malformations including anophthalmia, congenital heart defects, diaphragmatic hernia, alveolar capillary dysplasia, lung hypoplasia, and mental retardation. Am. J. Hum. Genet. *80*, 550–560.

Petkovich, M., Brand, N.J., Krust, A., and Chambon, P. (1987). A human retinoic acid receptor which belongs to the family of nuclear receptors. Nature *330*, 444–450.

Quadro, L., Blaner, W.S., Salchow, D.J., Vogel, S., Piantedosi, R., Gouras, P., Freeman, S., Cosma, M.P., Colantuoni, V., and Gottesman, M.E. (1999). Impaired retinal function and vitamin A availability in mice lacking retinol-binding protein. EMBO J. *18*, 4633–4644.

Tingaud-Sequeira, A., Forgue, J., Andre, M., and Babin, P.J. (2006). Epidermal transient down-regulation of retinol-binding protein 4 and mirror expression of apolipoprotein Eb and estrogen receptor 2a during zebrafish fin and scale development. Dev. Dyn. *235*, 3071–3079.

Weinberg, E.S., Allende, M.L., Kelly, C.S., Abdelhamid, A., Murakami, T., Andermann, P., Doerre, O.G., Grunwald, D.J., and Riggleman, B. (1996).

Developmental regulation of zebrafish MyoD in wild-type, no tail and spadetail embryos. Development *122*, 271–280.

Westerfield, M. (1994). The Zebrafish Book (Eugene, OR, USA: University of Oregon Press).

Xie, Y., Lashuel, H.A., Miroy, G.J., Dikler, S., and Kelly, J.W. (1998). Recombinant human retinol-binding protein refolding, native disulfide formation, and characterization. Protein Expr. Purif. *14*, 31–37.

Yang, Q., Graham, T.E., Mody, N., Preitner, F., Peroni, O.D., Zabolotny, J.M., Kotani, K., Quadro, L., and Kahn, B.B. (2005). Serum retinol binding protein 4 contributes to insulin resistance in obesity and type 2 diabetes. Nature *436*, 356–362.

Ziv, L., and Gothilf, Y. (2006). Circadian time-keeping during early stages of development. Proc. Natl. Acad. Sci. USA *103*, 4146–4151.